Available online at www.sciencedirect.com

ScienceDirect

Procedia Structural Integrity 28 (2020) 1193–1203

Structural Integrity Procedia

www.elsevier.com/locate/procedia

1st Virtual European Conference on Fracture

A cohesive-based method to bridge the strain rate effect and defects of RTM-6 epoxy resin under tensile loading

Dayou Ma[a], Ahmed Elmahdy[b], Patricia Verleysen[b], Marco Giglio[a], Andrea Manes[a,*]

[a]*Politecnico di Milano, Department of Mechanical Engineering, via la Masa, 1, 20156 Milan, Italy. dayou.ma@polimi.it, marco.giglio@polimi.it, andrea.manes@polimi.it*

[b]*Department of Electromechanical, Systems & Metal Engineering, MST-DyMaLab, Ghent University, Technologiepark 46, B-9052 Zwijnaarde, Belgium. ahmed.elmahdy@UGent.be, patricia.verleysen@UGent.be*

Abstract

The objective of the present work is to investigate the relationship between the strain rate effect of RTM-6 epoxy resin and the presence of defects under tensile loading by means of a numerical modelling approach. High-strain-rate tensile tests were conducted using a split Hopkinson tension bar (SHTB) test facility. Axial strains were locally measured within the gauge section of the sample using a high-speed stereo digital image correlation technique (high-speed 3D DIC). Additionally, quasi-static tensile tests were conducted to study the tensile behaviour over a wide range of strain rates. The dynamic experimental results showed an increase in strength and modulus, but also a noticeable reduction in the failure strain, compared to the quasi-static tests. Latter observation may be attributed to the effect of defects present in brittle polymeric materials. Defects lead to the generation of microcracks before the failure of samples, as confirmed by experimental observations. Two different cohesive models were therefore created to replicate the constitutive model of the material with and without defects. Through an inverse method fitting, the failure mechanism of cohesive elements was calibrated and the tensile behaviour at various strain rates was replicated. The results showed that the strain rate effect can be accurately simulated by implementing cohesive elements that mimic the presence of defects. The number of simulated defects that allows an accurate reproduction of the behaviour depends on the strain rate level and the material appears more sensitive to defects at high strain rates. Therefore, the present work validates the assumption of the relationship between strain rate effect and defects for brittle polymeric materials.

* Corresponding author. Tel.: +39-02-2399-8630; fax: +39-02-2399-8263.
E-mail address: andrea.manes@polimi.it

2452-3216
10.1016/j.prostr.2020.11.101

Keywords: epoxy resin; high strain rate; fracture mechanism; zero-thickness cohesive elements

1. Introduction

During the service life of polymer materials, tensile loading is hard to avoid, especially considering the fracture behaviour evoked by the tensile stress (Ma et al., 2020). However, the investigation of the tensile properties of polymer materials is complex because their mechanical properties varies due to the presence of very influential factors, such as material uncertainty (Li et al., 2020a), strain rate (Li et al., 2020b; Zotti et al., 2020) and inevitable defects (Zhou et al., 2005). The tensile behaviour of RTM-6, known as a highly cross-linked thermoset, commonly applied as coating and matrix of composites due to its high strength and temperature resistance, has been found to be complicated especially under various strain rates. A proper model, which replicates the tensile behaviour of RTM-6, is required. Such a model might be helpful in uncovering the potential mechanism of the strain rate effect on polymer materials.

Experimental investigations on the tensile properties of RTM-6 have been widely conducted at various strain rates. In quasi-static tests, RTM-6 epoxy resin presents a nonlinear behaviour after the yield stress (Chevalier et al., 2016; Morelle et al., 2017), but under dynamic conditions the tensile behaviour is totally different according to the work of Gerlach et al. (Gerlach et al., 2008), which focussed on the high strain rate response of RTM-6 epoxy resin using split Hopkinson tensile bar (SHTP) tests. A brittle behaviour, characterised by high strength and Young's modulus though low failure strain, can be obtained under high strain rates, while dynamic conditions lead to a reduction of nonlinearity. Such behaviour is not unique for thermoset polymers, e.g., PMMA has similar stress-strain curves under tension considering various strain rates (Wu et al., 2004), and therefore the investigation of the strain rate effect on the tensile mechanical property of RTM-6 epoxy resin can help to uncover a more generic mechanism.

Usually, during a tensile test, final fracture is preceded by microcracking. The observed stress-strain response is the result of both the materials' tensile and fracture behaviours. The analysis of the fracture behaviour during tension is thus of great importance, even though it is difficult due to the high speed of the fracturing process. However, with the recent development of detection methods, fracture during tension can be investigated, aided by digital image correlation (DIC) (Li et al., 2020a) and post analysis by microscopy (Morelle et al., 2017). The analysis of microscopy images of the fracture surface revealed that the defects of the brittle polymeric materials, which are inevitable due to the manufacturing process, are the main reason for the different behaviour under various strain rates (Zhou et al., 2005). Even though avoiding the effect of defects in tests on polymer materials is almost impossible, small samples are always used in related experiments to reduce the influence of defects.

As for the modelling strategies, a cohesive model is one of the most efficient methods to capture the facture and failure behaviours of materials. Cohesive models have been widely used for the simulation of the delamination in composite materials when applied to cohesive elements (Li et al., 2019) or contact models (Ma et al., 2019). The cohesive models are also usually used to model the interface, which does not physically exist, but has an essential effect on the results. Replication of cracks meets this application: a crack does not exist until a fracture initiates. Consequently, the cohesive model was able to mimic the crack in fracture tests with assistance of common elements (Tabiei and Zhang, 2018). Furthermore, a modified cohesive model can replicate the defected materials as conducted by Zhou et al. (Zhou et al., 2005). However, the drawback of the use of the cohesive model for crack replication is the extensive calculation cost because, considering the random nature of the crack generation, the cohesive model should be inserted between each two adjacent elements, which significantly increases the calculation time.

The objective of the present work is to investigate the tensile properties of RTM-6 epoxy resin under different strain rates and to create an in-depth understanding of the potential mechanism behind the strain rate effect through numerical modelling. For this purposes, tensile tests on small samples of RTM-6 epoxy resin with a SHTB facility were conducted in the present work and were monitored by high-speed DIC. This provides reliable experimental data of the strain rate effect, while the fracture behaviour can be captured by the high-speed cameras. Assuming that the strain rate effect can be attributed to activation of defects, a numerical model using zero-thickness cohesive elements was developed with two cohesive models for materials with and without defects assigned. Through controlling the number of defective cohesive elements, the tensile behaviour of RTM-6 epoxy resin under various strain rates can be replicated, which may validate the assumption that the strain rate effect is due to the activation of defects in brittle polymeric materials.

2. Materials and experimental methods

2.1. Specimen material and geometry

The RTM-6 epoxy resin used in this study was supplied by Hexcel composites. It consists of tetra-functional epoxy resin tetraglycidyl methylene dianiline (TGMDA), two hardeners 4,4′-methylenebis (2,6-diethylaniline) and 4,4′-methylenebis(2-isopropyl-6-methylaniline). Mixed resin and hardener were poured into long cylindrical rods which were then mechanically machined into small dog-bone samples. Threaded aluminum caps were glued on the shoulders of the dog-bone sample, in order to be gripped by the Hopkinson bars during testing. Figure 1 shows the dimensions of the RTM6 epoxy samples used, and a sample with threaded caps.

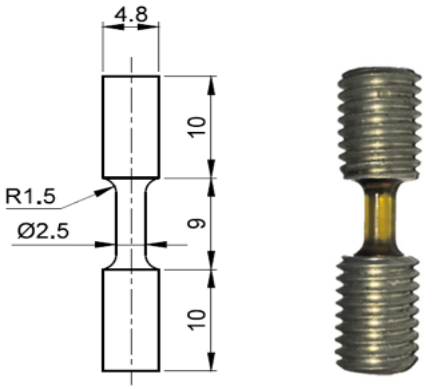

Figure 1 Dimensions of the tensile sample used (left) and image of the sample with the threaded caps (right)

2.2. Quasi-static and high strain rate setups

Referenced quasi-static tensile tests were performed using a Deben micro tensile testing stage. The load was measured using a 1000 N loadcell. Tensile tests were performed at a testing speed of 1mm/min. Local displacements and strains were measured on the surface of the samples using 3D digital image correlation technique. The optical setup consisted of two 5 megapixel cameras equipped with two fixed focus lenses of 100 mm focal length each. Samples were painted with a speckle pattern prior to testing. Figure 2 shows the quasi-static setup used.

High strain rate tensile tests were performed using the SHTB facility available at Ghent University. The setup consisted of two long aluminum bars (input and output bars) with the sample fixed in between. The diameter of the input bar was 25 mm while the diameter of the output bar was 12 mm. Small threaded end tabs were provided at the ends of both bars, in order to fix the tensile samples with the threaded caps. The average stress, strain and strain rate in the sample can be calculated from strain signals measured directly on the bars based on the one-dimensional wave propagation analysis. Additional details on the setup, the measurements, and the post processing of the data can be found in a previous work by Elmahdy et al. (Elmahdy and Verleysen, 2019). Similar to the quasi-static tests, local displacements and strains were measured using high speed stereo digital image correlation (high-speed 3D DIC). The system consisted of two Photron Mini AX200 high speed cameras, fitted with two fixed focus lenses of 90 mm focal length. Figure 3 shows the high strain rate setup used. Post processing of the images was performed using MatchID commercial software. The axial tensile strain was extracted from an area of 2x5 mm^2 around the center of the sample. The correlation criterion used for processing of the images was zero normalized sum of square differences (ZNSSD).

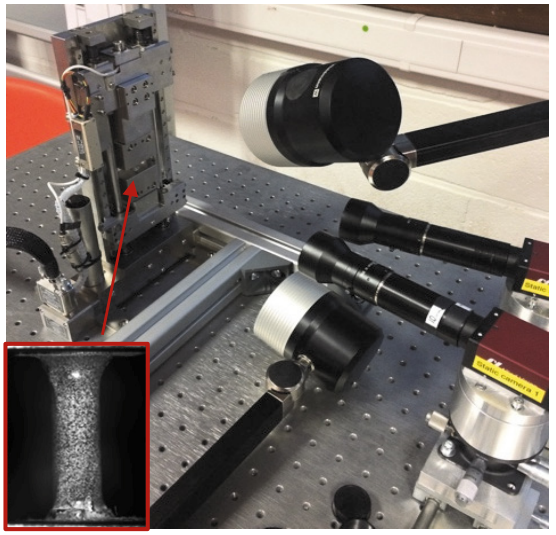

Figure 2 Quasi-static setup used with detail of the speckled sample (bottom left)

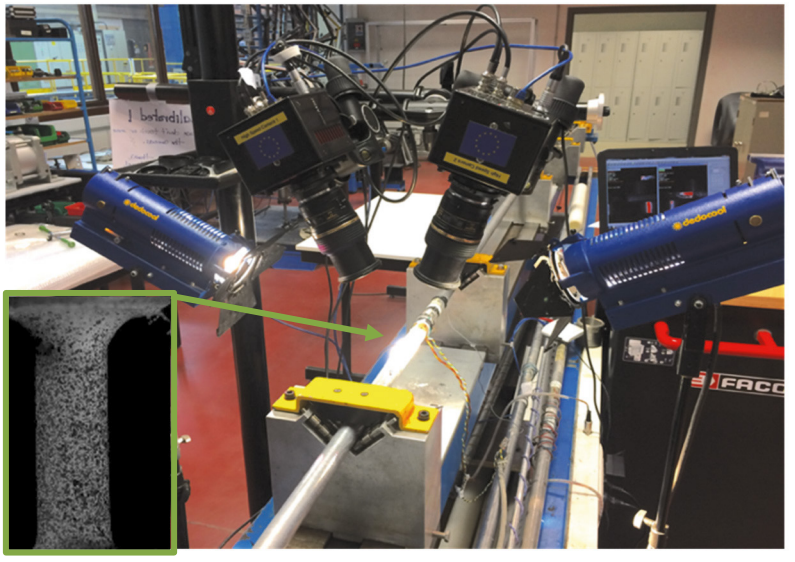

Figure 3 Experimental setups and the sample employed (static and dynamic)

2.3. Experimental results

Figure 4 shows an example of the engineering stress-engineering strain response of RTM-6 epoxy resin in tension at different strain rates. The solid lines indicate a second-degree polynomial fit, with R^2 values above 0.8. The achieved strain rates were in the range of 0.003 s^{-1} to 160 s^{-1}. The RTM-6 epoxy resin was strain rate sensitive in tension. Indeed, an increase of the strain rate led to an increase of the stiffness and strength of the epoxy but decreased the fracture strain. The tensile behavior of RTM-6 epoxy at the quasi-static range showed a highly non-linear response, compared to the nearly linear response at high strain rates. Similar behavior was also reported by Morelle et al. (Morelle et al., 2017) at quasi-static strain rates, and by Gerlach et al. (Gerlach et al., 2008) at high strain rates.

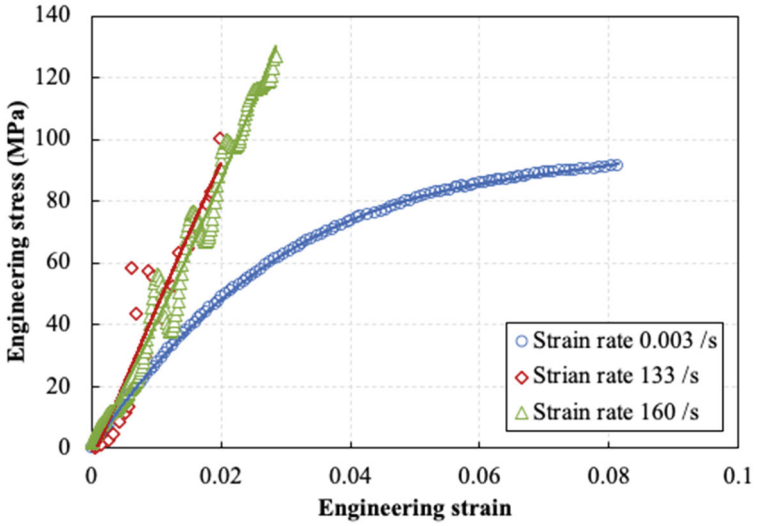

Figure 4 Experimental engineering stress-strain response of RTM6 epoxy tensile tests at various strain rates

3. Numerical approach

3.1. FE model

The finite element (FE) model used in the present work is presented in Figure 5. The centre of the gauge region of the tensile sample was modelled with a 2D model because the centre of the sample can be regarded as the main region representing the mechanical behaviour of the whole sample. The Belytschko-Tsay shell element was employed in the present model with a linear elastic model. To replicate the fracture behaviour of the RTM-6 epoxy resin, zero-thickness cohesive elements (ELFORM=29 in LS-DYNA) were inserted between each pair of the normal shell elements. In view that the fracture behaviour of the present work is controlled by the cohesive elements, no failure model was assigned to the shell elements for simplification. In the present work, two cohesive models were used for modelling the perfect material and material containing defects with more details provided in Section 3.3. Additionally, the loads applied on the sample was the displacement along y-axial, as shown in Figure 5, identical to the experimental activities and the FEM model was built through LS-DYNA.

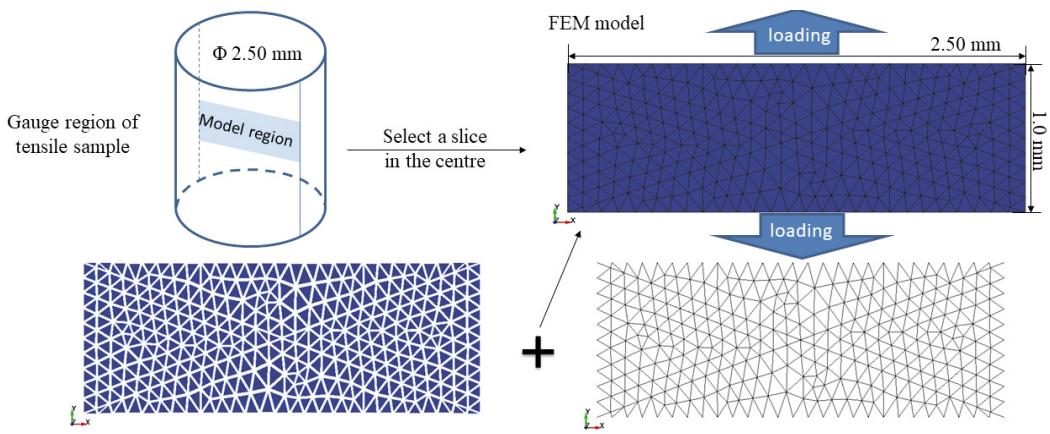

Figure 5 FE model for the present work

3.2. Mesh morphology

As presented in Figure 5, the mesh morphology was arbitrary in the model. Three typical mesh morphologies considered in the present work are listed in Figure 6. Cohesive elements were built to consider the effect of defects, which are formed randomly in the material and, hence, an arbitrary mesh was appropriate instead of a regular mesh. However, as the generation of the arbitrary mesh was uncontrollable, two mesh types, denoted as Mesh-A and Mesh-B in Figure 6, were obtained. According to the results from the tensile simulations with the two arbitrary mesh morphologies presented in Figure 6, the results on the tensile stress-strain curves with different arbitrary meshes are comparable. However, the more arbitrary mesh, i.e. Mesh-B, can provide better fracture predictions due to the random feature of the defects in polymer materials and, thus, Mesh-B was further employed.

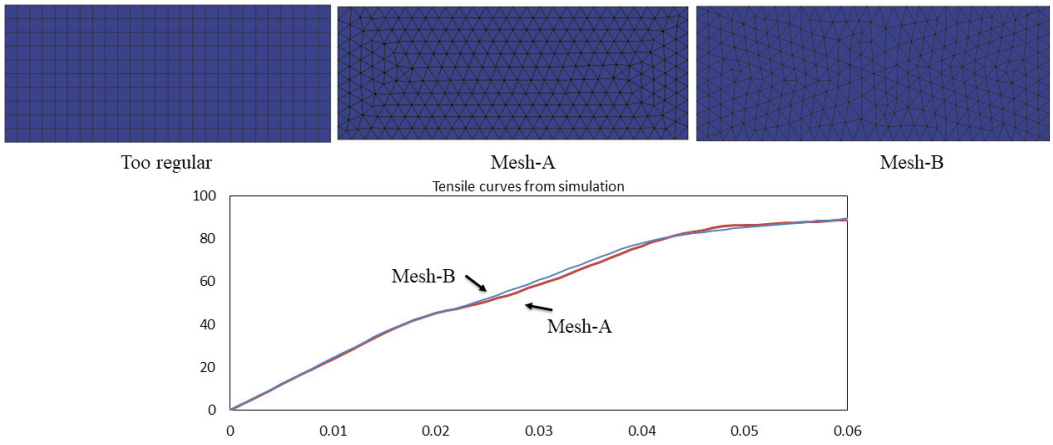

Figure 6 Study of the effect of various mesh morphologies

3.3. Material model

To study the relationship between the effect of the strain rate and defects, two different cohesive models were created to replicate the mechanical behaviour of the material without and with defects, as type-I and type-II presented in Figure 7, while the linear elastic material model was applied on the normal shell elements with Young's modulus and Poisson ratio equal to 2900 MPa and 0.36. Generally, G_c and σ_f are necessary to determine the shape of cohesive model, while ε_f can be calculated accordingly, therefore, only G_c and σ_f can be regarded as the input data in the present model. In the present work, cohesive models were built through MAT_186 (*MAT_COHESIVE_GENERAL) in LS-DYNA. The type-I cohesive model was used to capture the mechanical behaviour of the pure RTM-6 epoxy resin, in perfect condition without defects. The nonlinear behaviour, when $\Delta < \Delta_d$ in Figure 7, was used to capture the nonlinear behaviour of RTM-6 under quasi-static conditions. All related parameters were obtained through fitting of the experimental results with the quasi-static model. The type-II cohesive model is utilized to mimic the material with defects. Defects can always lead to a stress concentration, producing an immediate peak in the material behaviour, which is described as the initial peak in the material model, type-II cohesive model. The comparison of the two models showed that the type-II model has a quicker failure, *i.e.* $G_c > G_c^d$ ($\varepsilon_f > \varepsilon_f^d$) in Figure 7, to replicate the accelerated failure process due to the presence of defects. Furthermore, the defected cohesive model, i.e. the type-II cohesive model, did not describe the behaviour of the defect itself, but of the material containing defects without considering the exact amount of defects.

Regarding the parameters involved in the present cohesive models:
$\sigma_f = 200MPa, \tau_f = 47MPa, \alpha_0 = 0.5, \Delta_0 = 0.1, \Delta_d = 0.2, \Delta_f = 1, \Delta_f^d = 0.3, G_{IC} = 113\,J/m^2$ (Gerlach et al., 2008; Tserpes, 2011; Zotti et al., 2020), where τ_f is used to describe the shear strength of the cohesive elements and the shear behaviour was reproduced in the same way as tension behaviour. Herein, it is noted that the value of the failure stress, σ_f, is large because it is used to model the material in perfect condition, which is difficult to obtain. Therefore, the

largest value presented in literature under various conditions (Gerlach et al., 2008) was employed. Herein, the proportion of cohesive elements with the type-II cohesive model was altered to obtain the related change on the stress-strain curves and the fracture behaviour of the simulated results compared with the experimental results at various strain rates. Thus, the aim to bridge the effect of strain rate and defects can be achieved. Replaced by the proportion of defects, the effect of the strain rate can be estimated in the numerical model, indicating the model in the present work is time independent. As a result, the implicit solver was used to conduct all the calculations in the present study. It took around 10 min for each simulation with the implicit solver (single CPU of I7-875 K 2.93 GHz 4 core/8 threads and 16 GB RAM), which is more efficient and significantly reduces the calculation time compared to the explicit solver usually employed in numerical studies of strain rate.

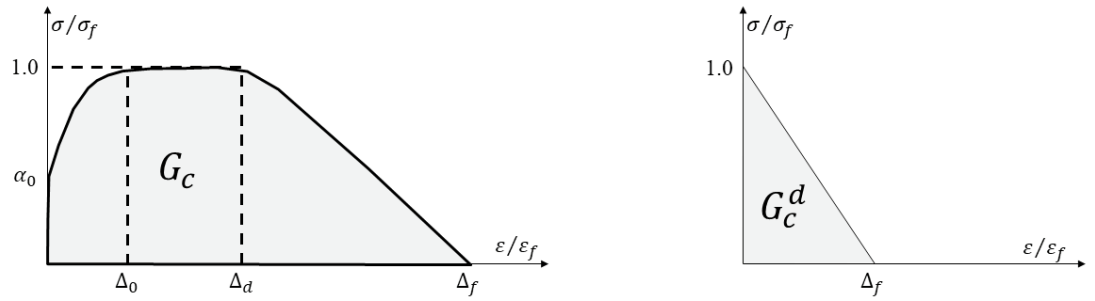

Figure 7 Cohesive models used in present work to present the material with (Type II) and without (Type I) the defects

4. Results and discussion

4.1. Effect of the proportion of defects

The simulated results of the stress-strain curves under tension with different proportions of the defective cohesive elements are shown in Figure 8. The peak stress and modulus increase with the increase of the proportion of defective cohesive elements. Additionally, the peak stress of the curves is actually smaller than the tensile strength of the cohesive model, indicating the shear failure is the main failure mechanism for the present work. A high proportion can reduce the nonlinearity in the numerical model. Furthermore, the trend of the change in the strength, modulus and nonlinearity with the proportion is identical to the change in those quantities with the strain rate, which provides feasibility to employ the proportion to replace the effect of strain rate in the numerical model.

4.2. Comparison with experimental data

No defective element was present in the model of the quasi-static case, *i.e.* 0% type-II cohesive elements. However, one single defective cohesive element was inserted into the centre to guarantee the crack initiation as the failure of RTM-6 epoxy resin always initiates from defects (Zhou et al., 2005). As presented in Figure 9, the tensile curve from the simulation showed good agreement with the experimental data, including in the nonlinear region. Regarding the fracture behaviour, a stable crack was found in the experiment, which can be replicated through the failure of the cohesive elements, as the crack path marked by the red line in Figure 9. In summary, the numerical results fitted the experimental data well with respects to the stress history and the fracture behaviour.

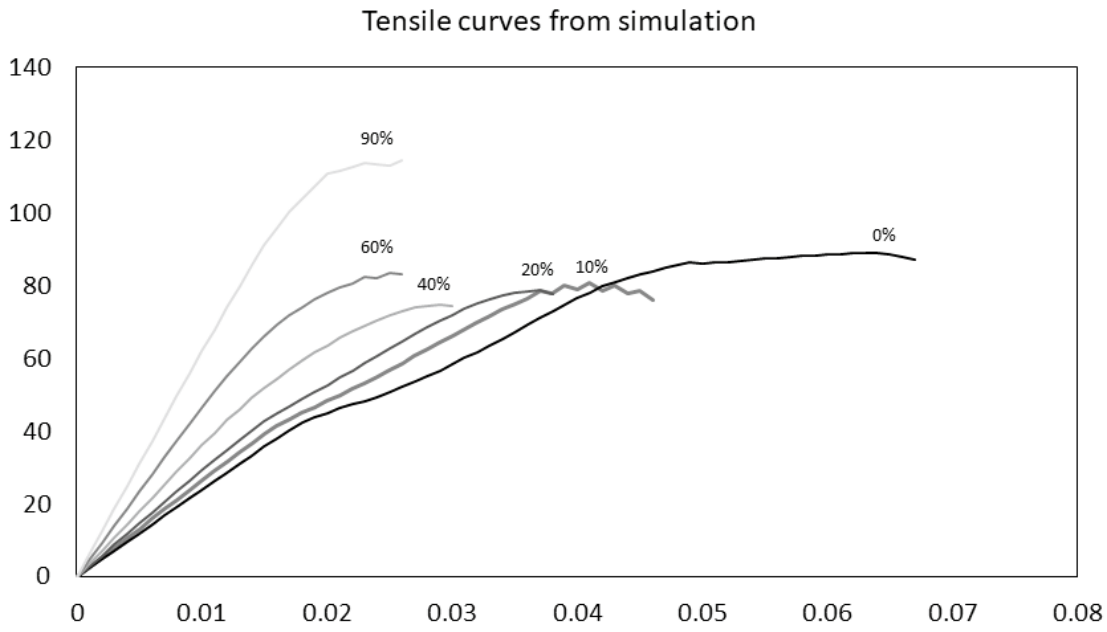

Figure 8 Stress-strain curves with different proportions of the defective cohesive elements

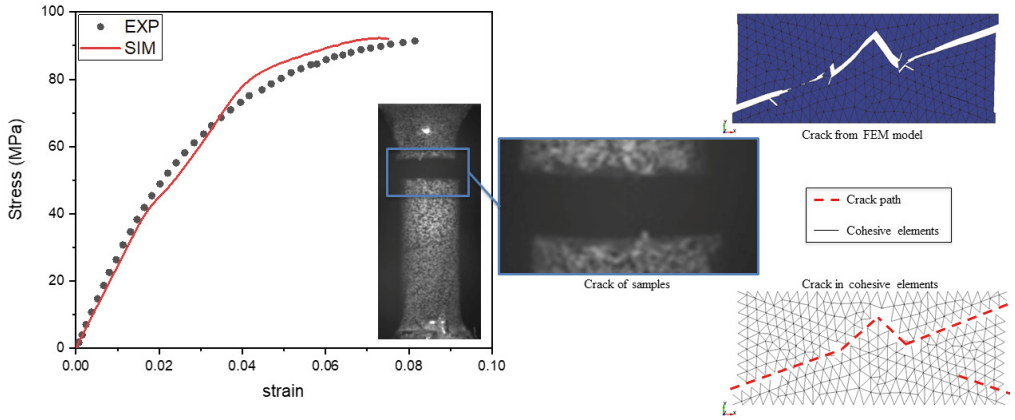

Figure 9 Comparison of tensile curves and fracture behaviour between the results from the numerical model and experiments for the quasi-static case

To obtain good agreement with the test results when the strain rate was equal to 133 /s, the proportion of randomly distributed defective cohesive elements should reach 80%. According to our investigation, the distribution only minimally affects the numerical results, so a typical case of the numerical model was selected for the comparison with the experimental data as shown in Figure 10. The tensile curve from the numerical model is comparable with the experimental curve. Considering the fracture behaviour, many discontinuous cracks were identified by the numerical model (marked as red lines in Figure 10). This phenomenon, denoted as “multi-cracks” in the present work, indicates that the failure was so unstable that more than one crack initiated. During the dynamic tests under this strain rate, two failure positions were recorded by the high-speed camera at the peak stress, which were also reported by Gerlach *et al.* (Gerlach et al., 2008) and can validate the multi-cracks predicted by the numerical model.

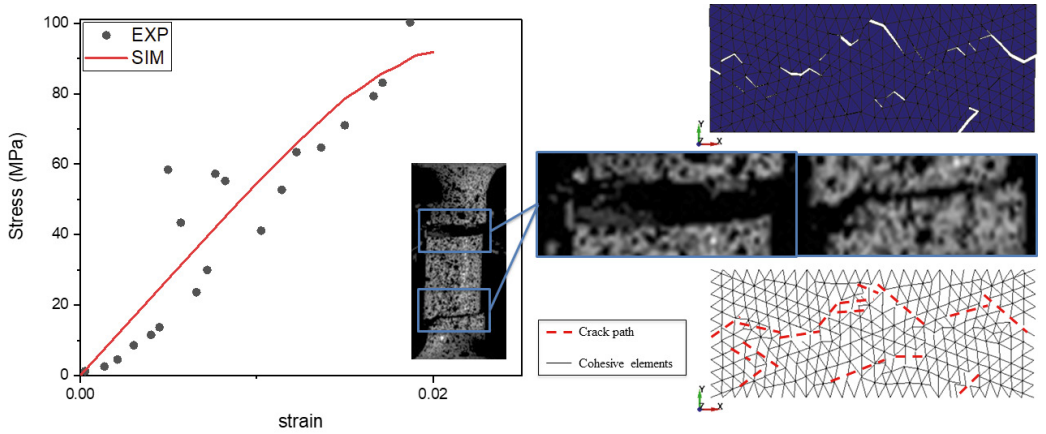

Figure 10 Comparison of the tensile curves and fracture behaviour between the results from the numerical model and experiments at a strain rate of 130 /s

The proportion of the defective cohesive elements should be 94% to fit the tensile curves with the strain rate equal to 160 /s. As presented in Figure 11, the stress-strain curves are in very close resemblance if the oscillations from the experimental data are ignored. Additionally, the phenomenon of multi-cracks was also obtained in the numerical results, see Figure 11. The fragments recorded and marked by red circles in Figure 11 confirmed the presence of the multi-cracks in the experiments. Considering all these comparable results, the present model is considered to be validated.

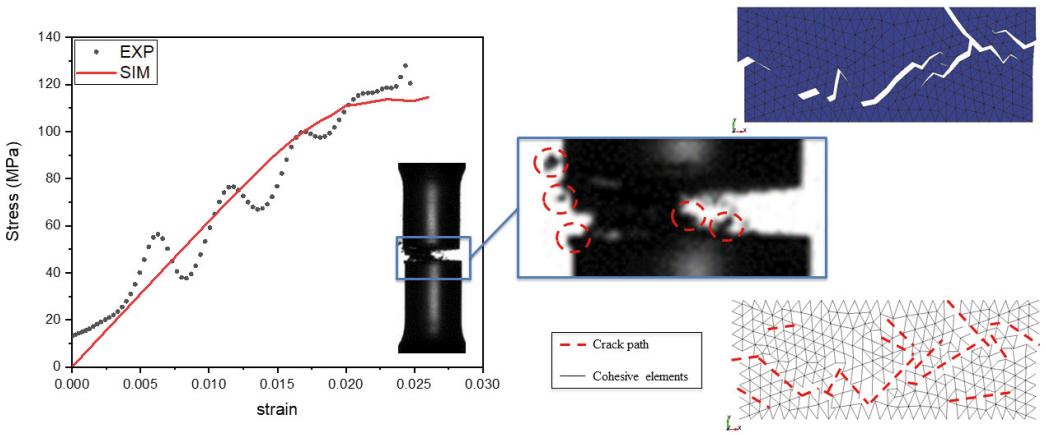

Figure 11 Comparison of the tensile curves and fracture behaviour between the results from numerical model and experiments under the strain rate of 160 /s

4.3. Discussion of the possible mechanism of the strain rate effect

The fracture surface was analysed through optical microscopic inspection (VHX-2000E, KEYENCE). As presented in Figure 12(a), the initiation of the failure of the RTM-6 epoxy resin was due to the existence of defects near the exterior surface, marked by a red circle. Similar phenomena were also reported in (Li et al., 2020b) for tensile tests. The presence of defects cannot be avoided, especially for polymer materials, regardless of the manufacturing process applied. As a result, defects are the key for the failure of the brittle polymeric materials. According to the results presented, the proportion of defects can be used to replicate the effect of the strain rate under tensile loading with respect to the stress-strain curves and the fracture phenomena. The obtained results can also be regarded as a validation

of the assumption of the relationship between the effect of strain rate and defects. The mechanical response of RTM-6 resin under different strain rates can be attributed to the existing defects: as the strain rate increases, the modulus increases according to the experimental stress-strain curves, indicating more energy absorbed by the material with the same strain level. Based on the present model considering defects, more energy can be absorbed as the increase of the proportion of defects, which fits the results from the experiments. Furthermore, the reduction of the nonlinearity can also correspond to the increasing amount of the activated defects, which may cause a quick failure. All of these indicate that high strain rate may activate more defects. Additionally, multi-cracks obtained from the numerical model, presented as more than one failure position or fragments during experimental tensile loading and observed as a change of the surface roughness shown in Figure 12(b), can also validate the previous explanation.

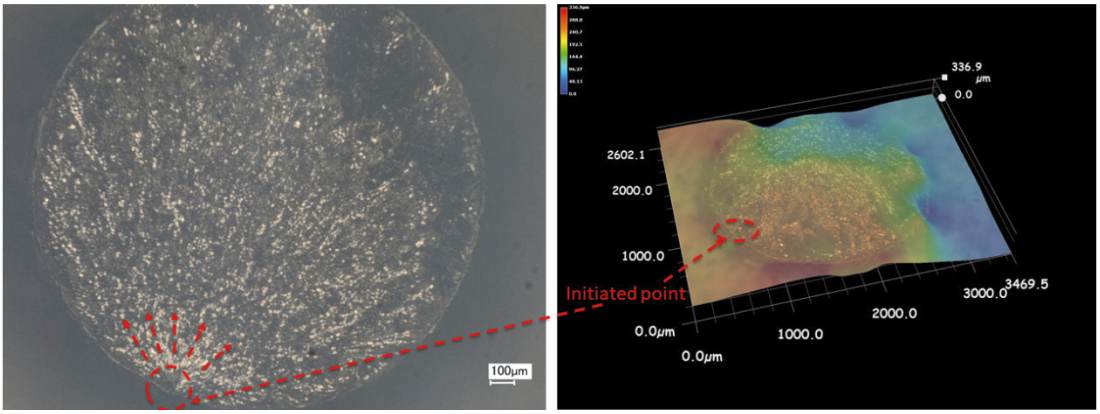

(a) (b)

Figure 12 Inspection of the fracture surface: (a) optical microscopy image; (b) roughness analysis

5. Conclusion

To bridge the effect of the strain rate and the defects, a numerical model was built in the present work with zero-thickness cohesive elements based on the experimental results of tensile tests under static and high strain rates. By changing the proportion of the defective cohesive model, the results from the numerical model can achieve good agreement with experimental data with respect to the stress-strain history and the fracture behaviour. The following main conclusions can be drawn:

- The fitting of the experimental curves, by means of the proportion of defective elements, shows that more defects seems to be activated as the test strain rate increases, which leads to more cracks prior to the collapse of the samples under high strain rates.
- As the amount of the defective cohesive elements increases, the strength and modulus increase while the failure strain decreases. Again, this is in a good agreement with the experimental results.
- The presence of defects seems to be one of the reasons for the strain rate effect of the brittle polymeric material (RTM-6 epoxy).

Additionally, to build a comprehensive numerical method, according to the present work further developments are still required to:

- Link the proportion of defective elements to physical parameters.
- Apply the method to complex loading conditions and large structures in order to check the transferability.

Acknowledgement

The authors would like to thank the Italian Ministry of Education, University and Research, through the project of the Department of Excellence LIS4.0 (Integrated Laboratory for Lightweight and Smart Structures). The experimental work was funded by the European Union's Horizon 2020 program through the EXTREME project, grant number 636549. Also, thanks are expressed to Dr. Aldobenedetto Zotti, Dr. Anna Borriello, and Dr. Mauro Zarrelli of the Italian Research Council-Institute of Polymers, Composites, and Biomaterials for providing the testing materials. A special thanks goes to Eliseo Hernández Durán, from Ghent University, for his valuable support for the microscopic inspection.

References

Chevalier, J., Morelle, X.P., Bailly, C., Camanho, P.P., Pardoen, T., Lani, F., 2016. Micro-mechanics based pressure dependent failure model for highly cross-linked epoxy resins. Eng. Fract. Mech. 158, 1–12. https://doi.org/10.1016/J.ENGFRACMECH.2016.02.039

Elmahdy, A., Verleysen, P., 2019. Tensile behavior of woven basalt fiber reinforced composites at high strain rates. Polym. Test. 76, 207–221. https://doi.org/10.1016/j.polymertesting.2019.03.016

Gerlach, R., Siviour, C.R., Petrinic, N., Wiegand, J., 2008. Experimental characterisation and constitutive modelling of RTM-6 resin under impact loading. Polymer (Guildf). 49, 2728–2737. https://doi.org/10.1016/J.POLYMER.2008.04.018

Li, X., Kupski, J., Teixeira De Freitas, S., Benedictus, R., Zarouchas, D., 2020a. Unfolding the early fatigue damage process for CFRP cross-ply laminates. Int. J. Fatigue 140, 105820. https://doi.org/10.1016/j.ijfatigue.2020.105820

Li, X., Ma, D., Liu, H., Tan, W., Gong, X., Zhang, C., Li, Y., 2019. Assessment of failure criteria and damage evolution methods for composite laminates under low-velocity impact. Compos. Struct. 207, 727–739. https://doi.org/10.1016/J.COMPSTRUCT.2018.09.093

Li, X., Saeedifar, M., Benedictus, R., Zarouchas, D., 2020b. Damage Accumulation Analysis of CFRP Cross-Ply Laminates under Different Tensile Loading Rates. Compos. Part C Open Access 100005. https://doi.org/10.1016/j.jcomc.2020.100005

Ma, D., Esmaeili, A., Manes, A., Sbarufatti, C., Jiménez-Suárez, A., Giglio, M., Hamouda, A.M., 2020. Numerical study of static and dynamic fracture behaviours of neat epoxy resin. Mech. Mater. 140, 103214. https://doi.org/10.1016/J.MECHMAT.2019.103214

Ma, D., Manes, A., Amico, S.C., Giglio, M., 2019. Ballistic strain-rate-dependent material modelling of glass-fibre woven composite based on the prediction of a meso-heterogeneous approach. Compos. Struct. 216, 187–200. https://doi.org/10.1016/j.compstruct.2019.02.102

Morelle, X.P., Chevalier, J., Bailly, C., Pardoen, T., Lani, F., 2017. Mechanical characterization and modeling of the deformation and failure of the highly crosslinked RTM6 epoxy resin. Mech. Time-Dependent Mater. 21, 419–454. https://doi.org/10.1007/s11043-016-9336-6

Tabiei, A., Zhang, W., 2018. A Zero Thickness Cohesive Element Approach for Dynamic Crack Propagation using LS-DYNA ®. pp. 1–15.

Tserpes, K.I., 2011. Strength Prediction of Composite Materials from Nano- to Macro-scale, in: Attaf, B. (Ed.), Advances in Composite Materials for Medicine and Nanotechnology. IntechOpen, Rijeka. https://doi.org/10.5772/13964

Wu, H., Ma, G., Xia, Y., 2004. Experimental study of tensile properties of PMMA at intermediate strain rate. Mater. Lett. 58, 3681–3685. https://doi.org/10.1016/j.matlet.2004.07.022

Zhou, F., Molinari, J.F., Shioya, T., 2005. A rate-dependent cohesive model for simulating dynamic crack propagation in brittle materials. Eng. Fract. Mech. 72, 1383–1410. https://doi.org/10.1016/j.engfracmech.2004.10.011

Zotti, A., Elmahdy, A., Zuppolini, S., Borriello, A., Verleysen, P., Zarrelli, M., 2020. Aromatic Hyperbranched Polyester/RTM6 Epoxy Resin for EXTREME Dynamic Loading Aeronautical Applications. Nanomaterials 10, 188. https://doi.org/10.3390/nano10020188